elements of the electric dipole operator p^k ($k = x, y, z$) to the one-electron matrix elements according to

$$I_r(\Delta E) \simeq \Delta E|\langle (E_0)\Gamma\gamma|p^k|(E_n)\Gamma'\gamma'\rangle|^2 = \Delta E|\sum A\langle \Gamma_1\gamma_1|p^k|\Gamma_2\gamma_2\rangle|^2$$

$|(E_0)\Gamma\gamma\rangle$ and $|(E_n)\Gamma'\gamma'\rangle$ are the ground- and excited-state wavefunctions of energies E_0 and E_n, respectively, with $\Delta E = E_n - E_0$, whereas A is a function of several group-theoretical coefficients and of nonvanishing one-electron dipole transition elements $\langle \Gamma_1\gamma_1|p^k|\Gamma_2\gamma_2\rangle$.[19]

In the d^7 configuration with a doublet ground state in the symmetry C_{2v} only the transition elements

$$p_z = \langle a_1(d_{z^2})|p^z|a_1(d_{x^2-y^2})\rangle$$

$$p_y^a = \langle a_1(d_{z^2})|p^y|b_2(d_{yz})\rangle \qquad p_y^b = \langle a_1(d_{x^2-y^2})|p^y|b_2(d_{yz})\rangle$$

$$p_x^a = \langle a_1(d_{z^2})|p^x|b_1(d_{xz})\rangle \qquad p_x^b = \langle a_1(d_{x^2-y^2})|p^x|b_1(d_{xz})\rangle$$

are nonvanishing and can be treated as parameters. The d functions in braces designate the main contribution to the relevant MO. In Table II the nonvanishing coefficients A are given for the different transitions calculated with a complete d^7 basis set in C_{2v} symmetry and strong-field coupling.[15] For the reduction of the number of parameters and for an estimate of relative intensities an SCCC calculation was performed for the CoN_6 polyhedra resulting in the relations

$$p_y^a \simeq 1.2p_y^b \qquad p_x^a \simeq -0.6p_x^b \qquad p_y^a = 1.6p_x^a$$

Atomic functions of $Co^+(3d, 4s, 4p)$ and $N(2p)$[9] were used without considering in-plane Co–N bonding. The overlap charges were partitioned according to Rein et al.[23] and based on the structural data, which were deduced from the available experimental results, in particular at low temperatures (compare the section in the Discussion concerning the low-spin state). The relations between the $p_k^{a,b}$ parameters are strongly dependent on the N–Co–N angles and the Co–N bond distances. Only a minor influence of the kind of approximation used for the calculation of the nondiagonal elements $\beta_{\mu\gamma}$ was found and thus justifies the neglect of the influence of the C atoms.

The relative intensities of the two transitions $^2A_1(a_1{}^2a_1) \rightarrow {}^2B_2(a_1a_1'b_2)$ and $^2B_1(a_1a_1'b_1)$ are calculated to be about 1 order of magnitude larger than the other ligand field bands. Hence it seems questionable whether the observed peaks at 17 800 and 19 200 cm^{-1} originate from d–d transitions. The intensity of the band at 7500 cm^{-1} mainly depends on the difference between the two axial Co–N bond lengths. This transition is extremely weak in the solution spectra and probably indicates a more regular $Co(terpy)_2{}^{2+}$ geometry than is observed in the solid compound. A similar decrease in the intensity of this transition is found for the corresponding $Cu(terpy)_2{}^{2+}$ ion, if one compares the reflection with the solution spectra.

(23) R. Rein, G. A. Clarke, and F. E. Harris, "Quantum Aspects of Heterocyclic Compounds in Chemistry and Biochemistry", Vol. II, Israel Academy of Sciences and Humanities, Jerusalem, 1970.

Contribution from the Institut für Physikalische und Theoretische Chemie and the Physikalisches Institut, Abt. II, University of Erlangen-Nürnberg, D-8520 Erlangen, West Germany, and the Department of Chemistry, The Queen's University of Belfast, Belfast BT9 5AG, Northern Ireland

The High-Spin ($^5T_2$) ⇌ Low-Spin ($^1A_1$) Transition in Solid Tris(2,2′-bi-2-imidazoline)iron(II) Diperchlorate. Hysteresis Effects, Simultaneous Change of Spin and Lattice Characteristics, and Order–Disorder Phenomena of the Perchlorate Anion

E. KÖNIG,*[1a] G. RITTER,[1a] S. K. KULSHRESHTHA,[1a,b] and S. M. NELSON[1c]

Received November 6, 1981

The sharp high-spin ($S = 2$; $^5T_2$) ⇌ low-spin ($S = 0$; $^1A_1$) transformation in solid $[Fe(bi)_3](ClO_4)_2$ (bi = 2,2′-bi-2-imidazoline) has been shown by variable-temperature ^{57}Fe Mössbauer-effect and X-ray diffraction measurements to be essentially of first order. The ground states involved are characterized, at the transition temperature $T_c\uparrow$, by $\Delta E_Q{}^I(^5T_2) = 2.42$ mm s^{-1}, $\Delta E_Q{}^{II}(^5T_2) = 1.99$ mm s^{-1}, $\delta^{IS}(^5T_2) = +1.09$ mm s^{-1} and $\Delta E_Q(^1A_1) = 0.22$ mm s^{-1}, $\delta^{IS}(^1A_1) = 0.42$ mm s^{-1}. A pronounced hysteresis of $\Delta T_c = 6.5$ K has been observed, the transition being centered at $T_c\uparrow = 114.8$ K for rising and at $T_c\downarrow = 108.3$ K for lowering temperature. The Debye–Waller factor shows a decrease of $\Delta f \approx 14\%$ at T_c, the temperature dependence of the effective thickness $t_{^5T_2}$ and $t_{^1A_1}$ being well reproduced within the high-temperature approximation of the Debye model ($\Theta_{^5T_2} = 133$ K for $T < 180$ K, $\Theta_{^5T_2} = 106$ K for $T > 200$ K; $\Theta_{^1A_1} = 190$ K; $M_{Fe} = 57$ au). The X-ray diffraction patterns for the $^5T_2$ and $^1A_1$ phases show characteristic differences. The Mössbauer spectra of the $^5T_2$ phase exhibit two doublets of almost equal intensity and different ΔE_Q values. At $T_2{}^{ClO_4} \approx 199$ K, a transformation into a single $^5T_2$ doublet ($\Delta E_Q = 1.70$ mm s^{-1} and $\delta^{IS} = +1.04$ mm s^{-1} at $T_c{}^{ClO_4}$) is observed. Changes of X-ray diffraction patterns suuggest a first-order character of the transition. The phenomenon is attributed to an order–disorder transition of the ClO_4 anion which will result in changes of the iron–nitrogen ligation. The two crystallographically inequivalent iron sites below $T_c{}^{ClO_4}$ correspond thus to two possible configurations of the ClO_4 anions.

Introduction

Temperature-induced high-spin ⇌ low-spin transitions in certain complexes of d^5, d^6, d^7, and d^8 transition-metal ions are well documented.[2] In solution, the spin interconversion process is dynamic in nature, and its mechanism seems to be

(1) (a) University of Erlangen-Nürnberg. (b) On leave of absence from Bhabha Atomic Research Center, Bombay, India. (c) Queen's University of Belfast.

(2) (a) For most recent reviews, see: H. A. Goodwin, *Coord. Chem. Rev.*, **18**, 293 (1976); (b) E. König, *Ber. Bunsenges. Phys. Chem.*, **76**, 975 (1972); (c) R. L. Martin and A. H. White, *Transition Met. Chem (N.Y.)*, **4**, 113 (1968); (d) P. Gütlich, *Struct. Bonding (Berlin)*, **44**, 83 (1981).

0020-1669/82/1321-3022$01.25/0

reasonably well understood.[3,4] The rate constants k_1 and k_{-1} for the process

$$\text{low-spin} \underset{k_{-1}}{\overset{k_1}{\rightleftharpoons}} \text{high-spin}$$

typically vary between 4×10^5 and 2×10^7 s^{-1}. In solid complexes, spin transitions are known to be of either an essentially discontinuous[5,6] or a more gradual[7] type. On the basis of heat capacity measurements,[8] the almost discontinuous transition in $[Fe(phen)_2(NCS)_2]$ and $[Fe(phen)_2(NCSe)_2]$ has been shown to be thermodynamically of first order (phen = 1,10-phenanthroline). It is generally believed that practically all spin transitions of the discontinuous type are first-order transitions, although the conclusive demonstration by heat capacity data is usually lacking. It should be noted that, according to the classification by Ehrenfest,[9] a transition is of the first order if discontinuous changes in volume and entropy are observed. Here, the entropy change is equivalent to the presence of a latent heat of transformation. In general, phase transitions of the first order exhibit hysteresis, which has therefore been often employed as an indication for this type of transition. It is of interest that the prototype of spin transitions in iron(II), $[Fe(phen)_2(NCS)_2]$, does not show any sign of hysteresis,[10] a fact that has been tentatively explained by the assumption of partial second-order character of the transition. Recently, the detailed study of hysteresis effects by a number of different physical methods, e.g. ^{57}Fe Mössbauer-effect, X-ray diffraction, and magnetic susceptibility measurements, has provided conclusive evidence for the simultaneous process of the change of metal ion spin state and the change of crystal lattice characteristics. This conclusion applies at least to the compounds studied thus far, i.e., $[Fe(phy)_2](ClO_4)_2$[11] (phy = 1,10-phenanthroline-2-carbaldehyde phenylhydrazone), $[Fe(bt)_2(NCS)_2]$[12] (bt = 2,2′-bi-2-thiazoline), and $[Fe(4,7\text{-}(CH_3)_2\text{-phen})_2(NCS)_2]$[13] (4,7-$(CH_3)_2$-phen = 4,7-dimethyl-1,10-phenanthroline).

However, the simple concept of a phase transition of first order has been complicated by various additional findings. Thus, in $[Fe(phy)_2](ClO_4)_2$, a transformation between the discontinuous and the gradual type of spin transition has been achieved by recrystallization of the sample.[11] Similar observations have been reported as a result of grinding and doping effects on the high-spin ($^6A_1$) ⇌ low-spin ($^2T_2$) transition in $[Fe(3\text{-}OCH_3\text{-SalEen})_2]PF_6$[14] (3-$OCH_3$-SalEen = monoanion of *N*-((ethylamino)ethyl)-3-methoxysalicylidenimine). In this context, the dilution studies on the spin transition complex $[Fe_xZn_{1-x}(2\text{-pic})_3]Cl_2 \cdot C_2H_5OH$[15] (2-pic = 2-picolylamine) should be mentioned. All these observations may be understood on the basis of domain formation and nucleation mechanisms.

In view of the recent progress in the field, additional investigations on spin transition systems are required, preferably on those of the discontinuous type. Some interesting observations have been recently presented[16] for the novel iron(II) complex $[Fe(bi)_3](ClO_4)_2$, where bi = 2,2′-bi-2-imidazoline:

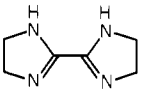

The effective magnetic moment of the compound of ca. 5.40 μ_B drops at ~115 K abruptly to assume a value of 0.59 μ_B at 93 K. On the basis of the obtained μ_{eff} values and preliminary ^{57}Fe Mössbauer spectra, it may be expected that the transition will be practically complete at both 293 and 93 K. In the present contribution we report, therefore, a more detailed study of the high-spin ($^5T_2$) ⇌ low-spin ($^1A_1$) transition in $[Fe(bi)_3](ClO_4)_2$ employing ^{57}Fe Mössbauer-effect and X-ray powder diffraction methods. In addition, the observation of an order–disorder transition is reported that is associated with the perchlorate anion in the compound.

Experimental Section

Materials. 2,2′-Bi-2-imidazoline as well as the samples of tris(2,2′-bi-2-imidazoline)iron(II) diperchlorate, $[Fe(bi)_3](ClO_4)_2$, were prepared as described elsewhere. All samples gave satisfactory analyses, their physical data being in agreement with those reported previously.[16]

Methods. ^{57}Fe Mössbauer spectra were measured with a spectrometer consisting of a constant-acceleration electromechanical drive and a Nuclear Data ND 2400 multichannel analyzer operating in the multiscaling mode. A 50-mCi source of ^{57}Co in rhodium was used, the calibration being effected with a metallic iron absorber. All velocity scales and isomer shifts are referred to the iron standard at 298 K. For conversion to the sodium nitroprusside scale, add +0.257 mm s^{-1}. Variable-temperature measurements were performed by using a custom-made superinsulated cryostat, the temperature being monitored by means of a calibrated iron vs. constantan thermocouple and a cryogenic temperature controller (Artronix Model 5301-E). The relative accuracy of temperature reading was about 0.05 K and the absolute accuracy about 0.5 K. The data were corrected for nonresonant background of the γ rays, and the individual areas A_i, i = ^1A, $^5T_2$, were extracted by a computer-based decomposition into Lorentzians. In this procedure, the positions and intensities of the individual peaks were treated as independent parameters, whereas a single line width was assigned to the two transitions originating from the same quadrupole doublet.

The effective thickness for the individual lines of the two phases, t_i, i = $^1A_1$, $^5T_2$, was obtained from the normalized area[17,18]

$$A_i = \tfrac{1}{2}\pi f_S \Gamma_0 [L(t_i)] \qquad (1)$$

In eq 1, f_S is the Debye–Waller factor of the source, Γ_i the line width of the absorber (in the present case $\Gamma_i = \Gamma_0$ where Γ_0 is the natural line width), and $L(t_i)$ the saturation function. The effective thickness is then determined, for $0 \le t_i \le 2$, with an accuracy greater than 1% according to

$$t_i(L) = L(t_i)/[1 - \tfrac{1}{4}L(t_i)] \qquad (2)$$

For the appropriate phase, the effective thickness follows the relation

$$t_{^5T_2} = d n_{^5T_2} f_{^5T_2} \qquad t_{^1A_1} = d(1 - n_{^5T_2}) f_{^1A_1} \qquad (3)$$

where $d = \tfrac{1}{2}N\beta\delta\sigma_0$, N being the number of iron atoms per unit volume, β the isotopic abundance, δ the absorber thickness, and σ_0 the resonance cross section. For the estimation of the high-spin fraction $n_{^5T_2}$, on the basis of eq 3, within the transition region, the quantity $f_{^5T_2}/f_{^1A_1}$ in that region is required. Below the transition, i.e., at temperatures where $n_{^5T_2} = 0$, it is $t_{^1A_1} = d f_{^1A_1}$. The measurements show that the high-temperature approximation for $f_{^1A_1}$ is applicable, whereby

$$-\ln t_{^1A_1} = -\ln d + LT \qquad (4)$$

(3) J. K. Beattie, R. A. Binstead, and R. J. West, *J. Am. Chem. Soc.*, **100**, 3044 (1978).
(4) R. A. Binstead, J. K. Beattie, E. V. Dose, M. F. Tweedle, and L. J. Wilson, *J. Am. Chem. Soc.*, **100**, 5609 (1978).
(5) E. König and K. Madeja, *Inorg. Chem.*, **6**, 48 (1967).
(6) E. König, G. Ritter, and B. Kanellakopulos, *J. Phys. C*, **7**, 2681 (1974).
(7) E. König, G. Ritter, W. Irler, and B. Kanellakopulos, *J. Phys. C*, **10**, 603 (1977).
(8) M. Sorai and S. Seki, *J. Phys. Chem. Solids*, **35**, 555 (1974).
(9) P. Ehrenfest, *Commun. Kamerlingh Onnes Lab. Univ. Leiden. Suppl.*, No. **36**, 153 (1933).
(10) P. Ganguli, P. Gütlich, E. W. Müller, and W. Irler, *J. Chem. Soc., Dalton Trans.*, 441 (1981).
(11) E. König, G. Ritter, W. Irler, and H. A. Goodwin, *J. Am. Chem. Soc.*, **102**, 4681 (1980).
(12) E. König, G. Rittrer, W. Irler, and S. M. Nelson, *Inorg. Chim. Acta*, **37**, 169 (1979).
(13) E. König, G. Ritter, and W. Irler, *Chem. Phys. Lett.*, **66**, 336 (1979).
(14) M. S. Haddad, W. D. Federer, M. W. Lynch, and D. N. Hendrickson, *Inorg. Chem.*, **20**, 131 (1981).
(15) M. Sorai, J. Ensling, and P. Gütlich, *Chem. Phys.*, **18**, 199 (1976).
(16) M. G. Burnett, V. McKee, and S. M. Nelson, *J. Chem. Soc., Dalton Trans.*, 1492 (1981).
(17) G. A. Bykov and Pham Zuy Hien, *Zh. Eksp. Teor. Fiz.*, **43**, 909 (1962).
(18) G. Lang, *Nucl. Instrum. Methods*, **24**, 425 (1963).

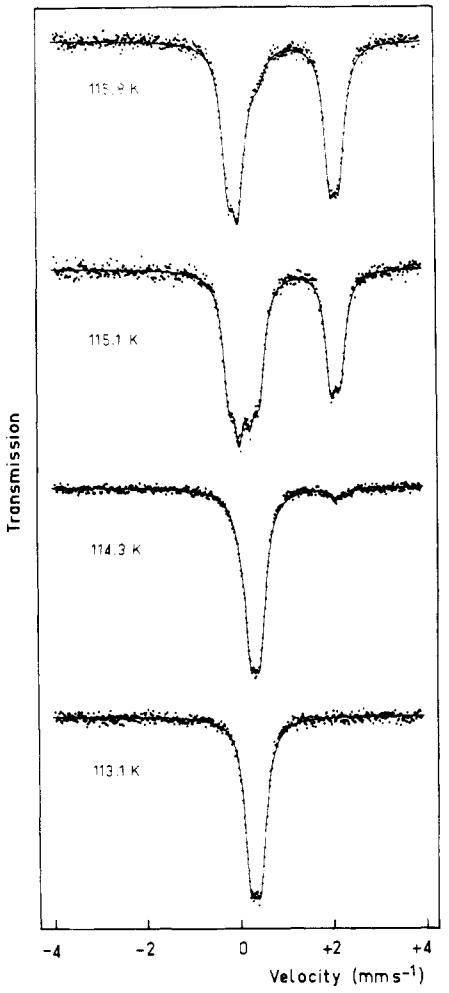

Figure 1. ^{57}Fe Mössbauer-effect spectra of $[Fe(bi)_3](ClO_4)_2$ at 113.1, 114.3, 115.1, and 115.8 K. The measurements were performed for increasing temperatures ($T_c\uparrow$ = 114.8 K).

Above the transition, i.e., where $n_{^5T_2} = 1$, $t_{^5T_2} = df_{^5T_2}$ holds. Similar to eq 4 we obtain

$$-\ln t_{^5T_2} = -\ln d + HT \tag{5}$$

where L and H are constant quantities. In the case of a very sharp transition between the two phases, as in the system studied at present, $-\ln t_{^1A_1}$ and $-\ln t_{^5T_2}$ may be extrapolated into the transition region. The ratio

$$\frac{t_{^5T_2}}{t_{^1A_1}} = \frac{f_{^5T_2}}{f_{^1A_1}} = \frac{e^{-HT}}{e^{-LT}} \tag{6}$$

deduced from eq 4 and 5 will now be valid also for the transition region. Consequently, this ratio may be employed to calculate indvidual values of $n_{^5T_2}$ from experimental values of $t_{^5T_2}$ and $t_{^1A_1}$ in the transition region with eq 3 as the basis.

Measurements of X-ray powder diffraction were performed with a Siemens counter diffractometer equipped with an Oxford Instruments CF 108A flow cryostat. Cu Kα radiation was used. Measurements of peak profiles were carried out in the mode of step scanning of the apparatus, the smallest steps being 0.005° in 2θ. The resulting pulses were stored and processed by a multichannel analyzer (Elscint MEDA 10). Temperatures were measured by a calibrated resistance thermometer, the relative accuracy being about 0.1 K.

Results

^{57}Fe Mössbauer Effect in the Region of Spin Transition Temperature. Two independently prepared samples of $[Fe(bi)_3](ClO_4)_2$ have been studied between 83.3 and 300.4 K. For the first of the samples, Figure 1 shows four typical spectra, i.e., at 113.1, 114.3, 115.1, and 115.8 K. The spectrum at 113.1 K is characterized by the quadrupole splitting ΔE_Q = 0.22 ± 0.01 mm s^{-1} and the isomer shift δ^{IS} = +0.43 ± 0.01 mm s^{-1}. At about 114.3 K, a second weak doublet becomes visible. If the temperature is increased further, the second doublet gains intensity, while the intensity of the first doublet is simultaneously decreasing; cf., e.g., the spectrum at 115.1 K in Figure 1. At 115.8 K, practically only the second spectrum is observed, whereby ΔE_Q = 2.20 ± 0.01 mm s^{-1} and δ^{IS} = +1.08 ± 0.01 mm s^{-1}. The Mössbauer spectra at and above 115.8 K are almost identical as are those at and below 113.1 K. The isomer shift of the spectrum at 113.1 K is characteristic for a low-spin $^1A_1$ ground state of iron(II), whereas that of the spectrum at 115.8 K is characteristic for a high-spin $^5T_2$ ground state. It is thus evident that the high-spin ($^5T_2$) ⇌ low-spin ($^1A_1$) transition for $[Fe(bi)_3](ClO_4)_2$ is very sharp and, for the first sample, almost 80% of the transition is completed within ~1.5 K, i.e., between 114.3 and 115.8 K. For the second sample, the transition was found to extend over the temperature range 113.1–117.5 K with the Mössbauer parameters identical with those for the first sample. On closer inspection of Figure 1 it is recognized that the high-spin part of the spectra is, in fact, composed of two high-spin doublets. At 115.8 K, e.g., decomposition into Lorentzians yields the values of quadrupole splitting for the two doublets as $\Delta E_Q^I(^5T_2)$ = 2.41 ± 0.01 mm s^{-1}, $\Delta E_Q^{II}(^5T_2)$ = 1.99 ± 0.01 mm s^{-1}, the value of 2.20 mm s^{-1} listed above being the average value. The isomer-shift values for the two doublets are identical within experimental uncertainty, viz., $\delta^{IS}(^5T_2)$ = +1.08 ± 0.01 mm s^{-1}. Detailed values of Mössbauer parameters for a number of representative temperatures are collected in Table I.

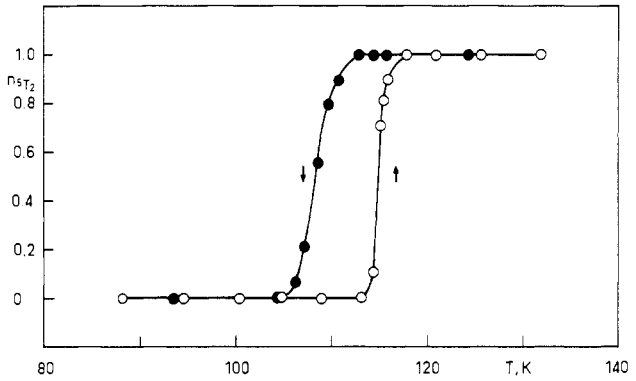

Figure 2. Temperature dependence of the high-spin fraction $n_{^5T_2}$ for $[Fe(bi)_3](ClO_4)_2$ on the basis of Mössbauer-effect measurements. The rising arrow indicates increasing temperatures, and the falling arrow indicates decreasing temperatures ($T_c\uparrow$ = 114.8 K, $T_c\downarrow$ = 108.3 K). Data collected with increasing temperatures are marked with open circles, and those obtained with decreasing temperatures are marked with filled circles.

If the temperature is decreased from above 120 K, the $^5T_2$ spectrum changes over into the $^1A_1$ spectrum at a temperature lower than has been observed for the $^1A_1 \rightarrow {}^5T_2$ transformation, i.e., when the sample is heated from below 113 K. This finding indicates that hysteresis effects are significant in $[Fe(bi)_3](ClO_4)_2$. The hysteresis associated with the high-spin ($^5T_2$) ⇌ low-spin ($^1A_1$) transition is illustrated in Figure 2 by plotting the high-spin fraction $n_{^5T_2}$, determined from the Mössbauer spectra, as a function of temperature. The temperature has been gradually increased from 100.3 to 125.6 K as indicated by the rising arrow. Subsequently, the temperature has been lowered as indicated by the falling arrow. Eventually, the initial temperature will be reached and thus the hysteresis loop is completed. The detailed values of $n_{^5T_2}$ are listed in Table II. The transition temperature T_c is usually defined by that temperature at which $n_{^5T_2}$ = 0.50. The transition is thus centered, for increasing temperatures, on $T_c\uparrow$ = 114.8 K, whereas for decreasing temperatures, $T_c\downarrow$ = 108.3

Table I. ^{57}Fe Mössbauer-Effect Parameters of $[Fe(bi)_3](ClO_4)_2$ for a Set of Representative Temperatures around the Spin Transition[a]

T, K	$\Delta E_Q(^1A_1)$,[b] mm s^{-1}	$\delta^{IS}(^1A_1)$,[c] mm s^{-1}	$\Delta E_Q^{I}(^5T_2)$,[b] mm s^{-1}	$\Delta E_Q^{II}(^5T_2)$,[b] mm s^{-1}	$\delta^{IS}(^5T_2)$,[c] mm s^{-1}
83.3	0.22	+0.43			
109.0	0.22	+0.42			
113.1	0.22	+0.43			
114.3	0.21	+0.42	2.16[d]		+1.12
115.1	0.21	+0.43	2.42	1.99	+1.09
115.4	0.24 ± 0.02	+0.41 ± 0.02	2.41	1.99	+1.07
115.8	0.28 ± 0.05	+0.41 ± 0.02	2.41	1.99	+1.08
117.8			2.41	1.97	+1.08
120.9			2.39	1.95	+1.08
115.7			2.40	1.98	+1.08
112.8			2.43	1.99	+1.08
110.7	0.28 ± 0.05	+0.36 ± 0.05	2.44	2.04	+1.08
109.7	0.21 ± 0.02	+0.43 ± 0.02	2.46	2.03	+1.09
108.5	0.21	+0.42	2.47	2.03	+1.09
107.1	0.21	+0.43	2.45	2.02	+1.10
106.3	0.21	+0.43	2.15[d]		+1.11
104.3	0.22	+0.42			
93.6	0.22	+0.42			

[a] The data are listed in the order of measurement. The values of $\Delta E_Q^{I}(^5T_2)$ and $\Delta E_Q^{II}(^5T_2)$ apply to two separate $^5T_2$ doublets of identical identical isomer shift $\delta^{IS}(^5T_2)$. [b] Experimental uncertainty ±0.01 mm s^{-1} except where stated. [c] Isomer shifts δ^{IS} are listed relative to that of natural iron at 298 K. The values for $\delta^{IS}(^5T_2)$ are the average values for the two separate $^5T_2$ doublets. Experimental uncertainty is ±0.01 mm s^{-1} except where stated. [d] Due to a very small value of $n^{5}T_2$, the spectrum was fitted with a single quadrupole doublet for the $^5T_2$ phase.

Table II. Effective Thickness t_i, i = $^1A_1$, $^5T_2$, and High-Spin Fraction $n^{5}T_2$ for $[Fe(bi)_3](ClO_4)_2$ in the Region of the Spin Transition Temperature[a]

T, K	$t^{1}A_1$	$t^{5}T_2$	$t^{5}T_2/(t^{5}T_2 + t^{1}A_1)$	$n^{5}T_2$
83.3	0.368			0
88.2	0.360			0
94.6	0.351			0
100.3	0.342			0
104.7	0.338			0
109.0	0.336			0
113.1	0.329			0
114.3	0.300	0.030	0.091	0.104
115.1	0.098	0.203	0.674	0.707
115.4	0.065	0.236	0.784	0.809
115.8	0.030	0.269	0.900	0.913
117.8		0.273	1.00	1.00
120.9		0.266	1.00	1.00
125.6		0.257	1.00	1.00
131.8		0.250	1.00	1.00
143.0		0.229	1.00	1.00
154.2		0.217	1.00	1.00
173.0		0.172	1.00	1.00
121.8		0.254	1.00	1.00
115.7		0.262	1.00	1.00
114.4		0.268	1.00	1.00
112.8		0.270	1.00	1.00
110.7	0.036	0.272	0.883	0.895
109.7	0.068	0.234	0.775	0.795
108.5	0.148	0.165	0.527	0.556
107.1	0.271	0.064	0.191	0.210
106.3	0.323	0.020	0.058	0.065
104.3	0.349			0
93.6	0.372			0

[a] The data are listed in the order of measurement.

K. The width of the hysteresis loop follows as 6.5 K. It should be noted that for the second sample, $T_c\uparrow$ = 115.1 K in good agreement with the first sample.

Values of the total effective thickness t_i, i = $^1A_1$, $^5T_2$, have been determined over the temperature range 83.3–300.4 K from the ^{57}Fe Mössbauer spectra as outlined in the Experimental Section. For increasing and for decreasing temperatures, t_i shows a discontinuity at $T_c\uparrow$ and $T_c\downarrow$, respectively, which corresponds to the change from $t_{^1A_1}$ to $t_{^5T_2}$ and vice versa. The results are illustrated in Figure 3, the individual values of t_i, i = $^1A_1$, $^5T_2$, being listed in Table II. It should be noted

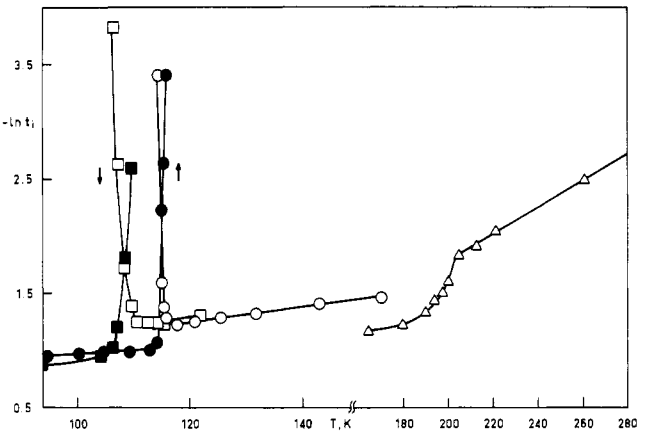

Figure 3. Temperature dependence of the effective thickness t_i, i = $^1A_1$ or $^5T_2$, for $[Fe(bi)_3](ClO_4)_2$ on the basis of Mössbauer-effect measurements. For details see the text. Filled symbols are used for the data of the $^1A_1$ ground state and open symbols for those of the $^5T_2$ ground state. The rising arrow indicates increasing temperatures (circles), and the falling arrow indicates decreasing temperatures (squares). Data for the region around $T_c^{ClO_4}$ (triangles) refer to measurements on an independent sample of different thickness.

that these t_i values correspond to one of the peaks for the low-spin $^1A_1$ phase and to the two or the one higher energy peaks for the high-spin $^5T_2$ phase below or above ~199 K, respectively. The temperature dependence of both $t_{^1A_1}$ and $t_{^5T_2}$ may be well reproduced within the high-temperature approximation of the Debye model

$$-\ln f_{T\geq\Theta/2} = \frac{3E_0^2}{Mc^2k\Theta}\left(\frac{T}{\Theta}\right) \qquad (7)$$

In eq 7, E_0 is the γ-ray energy (E_0 = 14.4 keV), Θ the Debye temperature, and for simple monoatomic lattices, M is identified with the mass of the absorbing atom (M_{Fe} = 57 au). Application to the experimental data gives, for both the samples

$$\Theta_{^1A_1} = 190 \pm 2 \text{ K}$$

$$\Theta_{^5T_2} = 133 \pm 2 \text{ K for } T < 180 \text{ K}$$

$$\Theta_{^5T_2} = 106 \pm 2 \text{ K for } T > 203 \text{ K}$$

Here, different values of $\Theta_{^5T_2}$ have been obtained for the

Table III. ^{57}Fe Mossbauer-Effect Parameters of $[Fe(bi)_3](ClO_4)_2$ for a Set of Representative Temperatures around the Order-Disorder Transition of the Perchlorate Anion

T, K	$\Delta E_Q^{I}(^5T_2)$,[a] mm s^{-1}	$\Delta E_Q^{II}(^5T_2)$,[a] mm s^{-1}	$\delta^{IS,I}(^5T_2)$,[b] mm s^{-1}	$\delta^{IS,II}(^5T_2)$,[b] mm s^{-1}	$t_{^5T_2}$
164.3	2.12	1.70	+1.07	+1.08	0.315
179.6	2.08	1.69	+1.05	+1.06	0.294
189.7	1.95	1.62	+1.04	+1.05	0.263
194.2	1.97	1.62	+1.04	+1.05	0.239
197.6	1.89	1.57	+1.03	+1.05	0.222
200.3	1.63		+1.04		0.200
204.6	1.57		+1.04		0.159
212.1	1.54		+1.03		0.149
221.0	1.49		+1.03		0.130
260.8	1.35		+1.01		0.083
285.1	1.24		+1.00		0.062

[a] Experimental uncertainty ±0.02 mm s^{-1}. [b] Isomer shifts δ^{IS} are listed relative to that of natural iron at 298 K. Experimental uncertainty is ±0.01 mm s^{-1}.

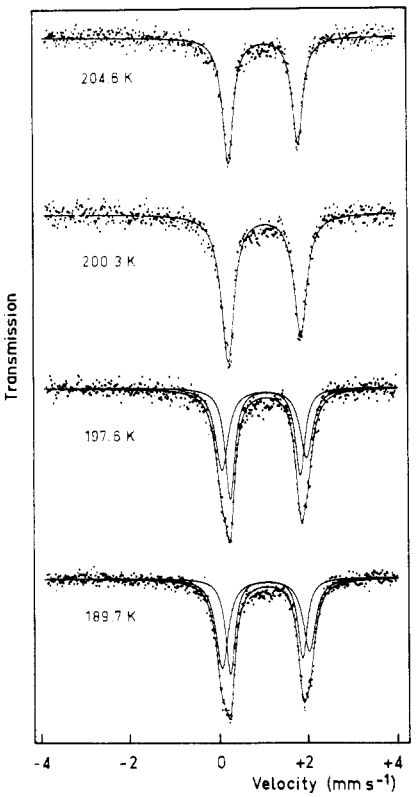

Figure 4. ^{57}Fe Mössbauer-effect spectra of $[Fe(bi)_3](ClO_4)_2$ around the temperature of the order–disorder transition of the ClO_4 ion ($T_c^{ClO_4} \approx 199$ K), i.e., at 189.7, 197.6, 200.3, and 204.6 K. The spectra include Lorentzian fits to a single doublet (at $T > T_c^{ClO_4}$) and the decomposition into two Lorentzian doublets (at $T < T_c^{ClO_4}$). The measurements were performed for increasing temperatures.

temperature ranges <180 K and >203 K, details being found in the next section.

For a test of the effect of fast cooling on the high-spin ($^5T_2$) ⇌ low-spin ($^1A_1$) transition, a sample of $[Fe(bi)_3](ClO_4)_2$ was quenched from room temperature to 77.6 K by directly dipping the sample into liquid nitrogen. Mössbauer spectra were subsequently recorded as a function of time. Initially, the sample showed the spectrum characteristic for the $^5T_2$ phase. As the time passed on, the $^1A_1$ doublet started appearing at the expense of the $^5T_2$ doublet, and in about 12 h, the transformation into the $^1A_1$ phase was almost complete. The Mössbauer parameters obtained from fitting of these spectra are $\Delta E^{I}(^5T_2) = 2.59$ mm s^{-1}, $\Delta E_Q^{II}(^5T_2) = 2.18$ mm s^{-1}, $\delta^{IS}(^5T_2) = +1.09$ mm s^{-1} and $\Delta E_Q(^1A_1) = 0.21$ mm s^{-1}, $\delta^{IS}(^1A_1) = +0.43$ mm s^{-1}. The values of the quadrupole splitting for the $^5T_2$ phase fit well into the curve for the temperature dependence of ΔE_Q (cf. Figure 5) if the curve is extrapolated to 77.6 K.

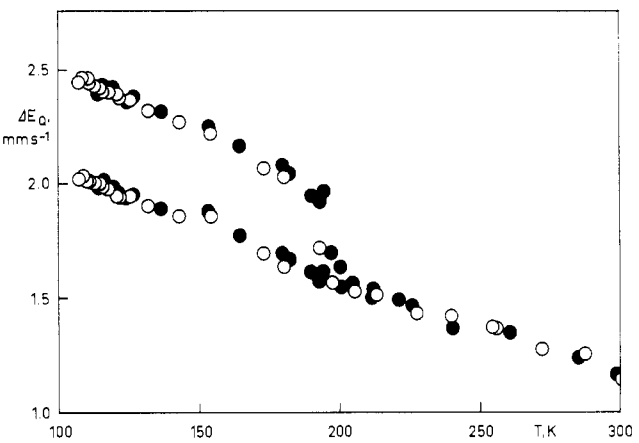

Figure 5. Temperature dependence of the quadrupole splitting ΔE_Q for the high-spin $^5T_2$ ground state of $[Fe(bi)_3](ClO_4)_2$. Two different sets of measurements are indicated as open and filled circles.

^{57}Fe Mössbauer Effect in the Region of the Order–Disorder Transition Temperature of the Perchlorate Anion. In the previous section it was demonstrated that, in the region of the high-spin ($^5T_2$) ⇌ low-spin ($^1A_1$) transition, the high-spin spectrum is formed of two overlapping $^5T_2$ doublets with slightly different values of ΔE_Q and almost equal intensity. The statement applies to all high-spin spectra between 115.1 and about 190 K. In Figure 4 it is illustrated how the two doublets of almost equal intensity collapse into a single quadrupole doublet at 200.3 K. The characteristic Mössbauer parameters of the $^5T_2$ doublet at 200.3 K, i.e., $\Delta E_Q = 1.63 \pm 0.02$ mm s^{-1} and $\delta^{IS} = +1.04 \pm 0.01$ mm s^{-1}, are similar to those for one of the doublets at lower temperature. Individual values of the Mössbauer parameters for a number of temperatures are listed in Table III. The behavior is illustrated, in addition, by the temperature variation of the quadrupole splitting ΔE_Q shown in Figure 5. This figure includes the ΔE_Q values of all Mössbauer spectra collected on the two samples of $[Fe(bi)_3](ClO_4)_2$. The agreement of the data is most gratifying. The transition between the two types of spectra likewise shows up in the temperature variation of the effective thickness $t_{^5T_2}$; cf. Figure 3. In particular, the values of the Debye temperature derived by application of eq 7 to measurements below and above the transition differ significantly, viz., $\Theta_{^5T_2} = 133$ K and $\Theta_{^5T_2} = 106$ K, respectively. The transition temperature is difficult to determine since there is a region rather than a single temperature of transition, viz., the interval 190–200 K. However, since the spectrum at 197.6 K is reasonably well fitted by two Lorentzian doublets, whereas that for 200.3 K is clearly represented by a single doublet (cf.

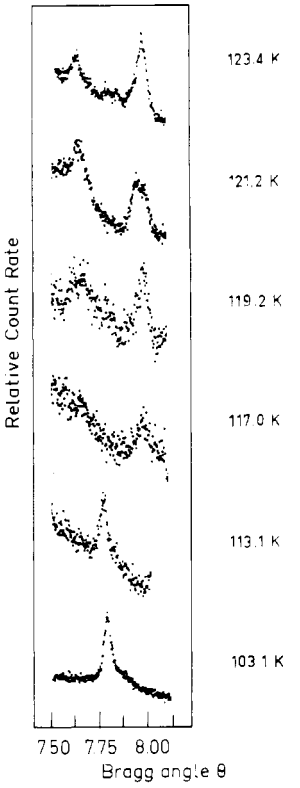

Figure 6. Peak profiles of X-ray powder diffraction for $[Fe(bi)_3](ClO_4)_2$ at temperatures between 103.1 and 123.4 K. The measurements were performed for increasing temperatures.

Figure 4), we assume that $T_c^{ClO_4} \approx 199$ K. As will be discussed below, the transition is attributed to order-disorder phenomena of the perchlorate anion in $[Fe(bi)_3](ClO_4)_2$.

Temperature Dependence of X-ray Diffraction Peak Profiles. The temperature dependence of peak profiles of the X-ray diffraction pattern of $[Fe(bi)_3](ClO_4)_2$ was studied between 99.8 and 300 K as described in the Experimental Section. The change with temperature is exemplified in Figure 6 for a particularly intense and well-defined powder peak. In the low-temperature region, i.e., at and below 113.1 K, a single peak is found for a diffraction angle $\theta = 7.83°$, and this peak is assigned to the $^1A_1$ ground state on the basis of Mössbauer spectra. At 117.0 K, two new powder peaks show up at about $\theta = 7.68$ and 8.00°, and these are attributed to the $^5T_2$ ground state, again with the Mössbauer spectra taken as a reference. With increasing temperature, the intensity of the peaks at 7.68 and 8.00° rises whereas that of the 7.83° peak simultaneously falls until, at and above 121.2 K, the diffraction pattern is characterized by the $^5T_2$ peaks alone. From the figure it is also apparent that, in the transition region, the X-ray diffraction peaks are relatively broad and ill-defined, whereas, as the transition is completed on either side, the peaks become quite narrow and well-defined. It should be noted that any differences in the temperatures listed for X-ray diffraction and Mössbauer-effect measurements are partly due to different temperature control equipment, the data from Mössbauer work being the more accurate, and the fact that the second sample has been employed for the X-ray diffraction study.

If the X-ray diffraction is followed by gradually lowering the temperature, the high-spin ($^5T_2$) $\rightleftharpoons$ low-spin ($^1A_1$) transition is found to take place at a temperature lower than that with increasing temperature. The sample thus shows crystallographic hysteresis effects at the transition. A quantitative analysis of the X-ray data within the region of hysteresis as in some previous studies[11,13] was not attempted due to the fact that it was not possible to locate the Bragg reflections corresponding to the same Miller indices in the two phases.

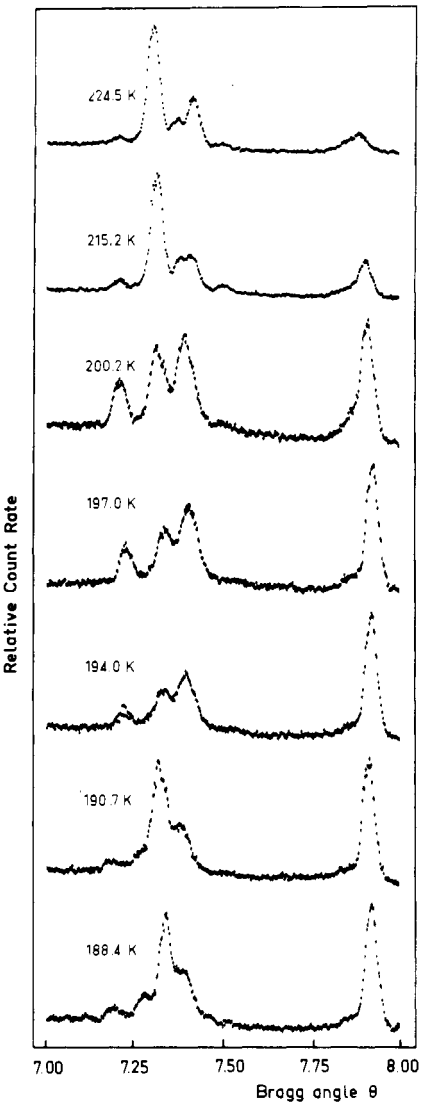

Figure 7. Peak profiles of X-ray powder diffraction for $[Fe(bi)_3](ClO_4)_2$ in the vicinity of the temperature of the order–disorder transition of the ClO_4 ion ($T_c^{ClO_4} \approx 199$ K), i.e., between 188.4 and 224.5 K. The measurements were performed for increasing temperatures.

For the study of the crystallographic changes associated with the order–disorder transition of the perchlorate anion, X-ray powder diffraction patterns were recorded for a number of temperatures in the vicinity of $T_c^{ClO_4}$. A typical set of X-ray powder peak profiles for temperatures between 188.4 and 224.5 K and for values of the diffraction angle θ between 7.0 and 8.0° is displayed in Figure 7. It is apparent that the diffraction patterns for temperatures above and below $T_c^{ClO_4}$ are significantly different in both position and intensity of several characteristic peak profiles. Note that temperatures of 194.0, 197.0 and 200.2 K apply to the transition region. Similar changes were also encountered for diffraction patterns collected in the region $10.5° \leq \theta \leq 13.0°$.

Discussion

The High-Spin ($^5T_2$) $\rightleftharpoons$ Low-Spin ($^1A_1$) Transition. It has been mentioned above that, according to the conventional thermodynamic classification,[9] a transition of first order is characterized by a discontinuous change of volume and entropy, i.e., a latent heat. In the case of $[Fe(bi)_3](ClO_4)_2$, a discontinuous change of volume at the transition temperature may be inferred from the study of X-ray diffraction and the discontinuity in the temperature dependence of the total effective thickness t_i, which is closely related to the Debye–

Waller factor f_i of the corresponding phase. In particular, it has been demonstrated that the Debye temperatures $\Theta_{^5T_2}$ and $\Theta_{^1A_1}$ are significantly different, which implies that the phonon spectrum will be different for the two phases, thus indicating a crystallographic rearrangement of the lattice at T_c. We have shown[12,19] that the almost discontinuous high-spin ($^5T_2$) $\rightleftharpoons$ low-spin ($^1A_1$) transition in $[Fe(bt)_2(NCS)_2]$, where bt = 2,2′-bi-2-thiazoline, and $[Fe(4,7\text{-}(CH_3)_2\text{-phen})_2(NCS)_2]$, where phen = 1,10-phenanthroline, may be rationalized in terms of a Bragg and Williams type model.[20] This interpretation is equally well applicable to the spin transition in $[Fe(bi)_3](ClO_4)_2$ and requires a latent heat and a change in entropy. On the basis of these facts it is suggested that the observed high-spin ($^5T_2$) $\rightleftharpoons$ low-spin ($^1A_1$) transition in $[Fe(bi)_3](ClO_4)_2$ should be considered as a transition of first order.

An additional characteristic property of phase transitions of first order are hysteresis effects, and indeed, a pronounced hysteresis of width $\Delta T_c = 6.5$ K has been found for $[Fe(bi)_3](ClO_4)_2$ in the Mössbauer-effect measurements. It should be noted that hysteresis associated with spin transitions in compounds of iron(II) has been reported for $[Fe(4,7\text{-}(CH_3)_2\text{-phen})_2(NCS)_2]$,[13,19] $[Fe(paptH)_2](NO_3)_2$ (paptH = 2-(2-pyridylamino)-4-(2-pyridyl)thiazole),[21] $[Fe(2\text{-pic})_3]Cl_2\cdot H_2O$,[22] $[Fe(bt)_2(NCS)_2]$,[12] and $[Fe(phy)_2](ClO_4)_2$.[11] Detailed studies of hysteresis effects may provide quite specific information about the mechanism of the phase transition if a model developed by Everett[23-25] is applied. This has been recently demonstrated for $[Fe(phy)_2](ClO_4)_2$.[11] In the present case, the required determination of scanning curves for $[Fe(bi)_3](ClO_4)_2$ has not been successful. Due to the extremely sharp nature of the transition we were unable to reproduce the same value of $t_{^5T_2}$ at the corresponding temperature during subsequent heating and cooling cycles since the slope of the two branches of the hysteresis loop became successively less steep. The most likely reason for this observation is cracking of the crystallites during the high-spin $\rightleftharpoons$ low-spin transition, which will introduce more surface defects every time. It may be mentioned that a similar behavior was noticed in magnetic susceptibility measurements.

Order–Disorder Transition of the Perchlorate Anion and Its Effect on the ^{57}Fe Mössbauer Spectra. On the basis of the Mössbauer spectra, a distinct transition is observed in $[Fe(bi)_3](ClO_4)_2$ at the temperature $T_c^{ClO_4} \approx 199$ K, whereby the two separate high-spin $^5T_2$ doublets found at $T < T_c^{ClO_4}$ collapse into a single $^5T_2$ doublet above $T_c^{ClO_4}$. The effective thickness shows a characteristic change (cf. Figure 3), and the values of the Debye temperature $\Theta_{^5T_2}$ above and below $T_c^{ClO_4}$ are significantly different. In addition, it has been shown above that crystallographic changes are associated with the transition. As in the case of the high-spin ($^5T_2$) $\rightleftharpoons$ low-spin ($^1A_1$) transition, these observations indicate that the transition is of first order.

A related observation, as far as Mössbauer spectra are concerned, has been made in the compound $[Fe(2\text{-}CH_3\text{-phen})_3](ClO_4)_2$ where a considerable broadening of the Mössbauer lines was encountered for the $^5T_2$ phase.[26] This compound is involved in a very gradual high-spin ($^5T_2$) $\rightleftharpoons$ low-spin ($^1A_1$) transition. Subsequently, the lines were resolved by Fleisch et al.[27] into two separate $^5T_2$ doublets over the entire temperature range between 4.2 and 295 K. The two doublets have been attributed to two different lattice sites of high-spin iron(II) characterized by a reversal of the orbital ground state, viz., $^5A_1$ and ^5E, of D_3 symmetry. It has been suggested that the two sites might originate in order–disorder phenomena of the ClO_4 anion. Indeed, it should be noted[26,28] that the line-broadening effect and thus the existence of two $^5T_2$ doublets are not observed if a different anion is involved; cf. the compounds $[Fe(2\text{-}CH_3\text{-phen})_3]X_2$, where X = BF_4, BPh_4, I.

Phase transitions in conjunction with order–disorder phenomena of the ClO_4 ion have been observed in various compounds. Particularly well studied, by various physical methods, have been these transitions in $[Me(H_2O)_6](ClO_4)_2$ complexes. Thus, in $[Fe(H_2O)_6](ClO_4)_2$, an iron(II) Mössbauer spectrum with $\Delta E_Q = 3.4$ mm s^{-1} has been reported for $T < 223$ K, whereas a spectrum characterized by $\Delta E_Q = 1.4$ mm s^{-1} has been found for $T > 253$ K, there being a region of coexistence of the two phases for $223 \leq T \leq 253$ K.[29] Mössbauer-effect measurements in an external magnetic field have shown[30] that a change of V_{zz} is involved. The transition thus proceeds, with increasing temperature, from a compression to an elongation of the coordination polyhedron. Raman contour measurements on ClO_4 bands in $[Ni(H_2O)_6](ClO_4)_2$ and $[Mg(H_2O)_6](ClO_4)_2$ revealed picosecond-rate stochastic reorientations or large-scale anharmonic librations of the ClO_4 ions at high temperatures.[31] These motions stop in the phase-transition region. Of relevance are X-ray diffraction studies on $[Ti(urea)_6](ClO_4)_2$ that show that at 300 K two of the oxygen atoms of the ClO_4 anions are disordered between two different sites.[32] The disorder is energetically favored since the oxygen atoms may form stronger hydrogen bonds to the urea nitrogens. At 90 K, the disorder has disappeared.[33] In $Fe^{II}(N,N'\text{-dicyclohexylthiourea})_6(ClO_4)_2$, Mössbauer measurements[34] have disclosed the existence of two phases, one phase being observed at $T < 200$ K with $\Delta E_Q = 3.31$ mm s^{-1}, the second phase at $T > 300$ K with $\Delta E_Q = 1.32$ mm s^{-1}. There is a coexistence region for $200 < T < 300$ K. The results have been interpreted by the temperature dependence of perchlorate disorder and a consequent variation of hydrogen bonding between the ClO_4 anions and the thiourea amine nitrogens, which should affect the metal–sulfur ligation.

In the present case of the 199 K transition in $[Fe(bi)_3](ClO_4)_2$, the possibility of hydrogen bonding between the ClO_4 anions and the NH groups of the 2,2′-bi-2-imidazoline ligands has to be considered. Indeed, alterations of the ligand field induced by these hydrogen bonds have been invoked[16] in order to explain the fully high-spin character of $[Fe(bi)_3](PBh_4)_2$. It has been ascertained on the basis of Mössbauer measurements that a transition of the type discussed here is not observed in $[Fe(bi)_3](BPh_4)_2$. By analogy to the results referred to above we suppose that the ClO_4 anions are hydrogen bonded and disordered in the high-temperature region. At $T_c^{ClO_4} \approx 199$ K, the disorder is frozen out and each perchlorate may assume one or the other of two possible configurations. The transition will involve subtle perturbations of the coordinated nitrogen atoms, and thus small changes of the Fe–N ligation

(19) E. König and G. Ritter, *Solid State Commun.*, **18**, 279 (1976).
(20) C. P. Slichter and H. G. Drickamer, *J. Chem. Phys.*, **56**, 2142 (1972).
(21) G. Ritter, E. König, W. Irler, and H. A. Goodwin, *Inorg. Chem.*, **17**, 224 (1978).
(22) M. Sorai, J. Ensling, K. M. Hasselbach, and P. Gütlich, *Chem. Phys.*, **20**, 197 (1977).
(23) D. H. Everett and W. I. Whitton, *Trans. Faraday Soc.*, **48**, 749 (1952).
(24) D. H. Everett and F. W. Smith, *Trans. Faraday Soc.*, **50**, 187 (1954).
(25) D. H. Everett, *Trans. Faraday Soc.*, **50**, 1077 (1954); **51**, 1551 (1955).
(26) E. König, G. Ritter, H. Spiering, S. Kremer, K. Madeja, and A. Rosenkranz, *J. Chem. Phys.*, **56**, 3139 (1972).
(27) J. Fleisch, P. Gütlich, K. M. Hasselbach, and W. Müller, *Inorg. Chem.*, **15**, 958 (1976).
(28) E. König, G. Ritter, B. Braunecker, K. Madeja, H. A. Goodwin, and F. E. Smith, *Ber Bunsenges. Phys. Chem.*, **76**, 393 (1972).
(29) L. Dezsi and L. Keszthelyi, *Solid State Commun.*, **4**, 511 (1966).
(30) W. M. Reiff, R. B. Frankel, and C. R. Abeledo, *Chem. Phys. Lett.*, **22**, 124 (1973).
(31) J. M. Janik, A. Migdal-Mikuli, E. Mikuli, and T. Stanek, *Acta Phys. Pol. A*, **a59**, 599 (1981).
(32) B. N. Figgis, L. G. B. Wadley, and J. Graham, *Acta Crystallogr., Sect. B*, **B28**, 187 (1972).
(33) B. N. Figgis and L. G. B. Wadley, *Aust. J. Chem.*, **25**, 2233 (1972).
(34) R. Latorre, C. R. Abeledo, R. B. Frankel, J. A. Costamagna, W. M. Reiff, and E. Frank, *J. Chem. Phys.*, **59**, 2580 (1973).

may result that will produce two different iron sites. In view of the small difference of the two ΔE_Q values, *viz.*, ΔE_Q^{I} = 2.41 mm s^{-1} and ΔE_Q^{II} = 1.99 mm s^{-1} at 115.1 K, and the identical temperature dependence of the quadrupole splitting, both iron(II) atoms will have presumably the same $^5A_1$ ground state. In contrast to several related transitions,[27,30,34] an orbital ground-state reversal may thus be ruled out for $[Fe(bi)_3](ClO_4)_2$. In the low-spin $^1A_1$ phase, the inequivalence of the two iron sites is not resolved due to the much smaller value of $\Delta E_Q(^1A_1)$, which is insensitive to lattice distortions.

Acknowledgment. The authors appreciate financial support by the Stiftung Volkswagenwerk and the Fonds der Chemischen Industrie. Thanks are also due to Dr. V. McKee for her assistance in the preparation of the samples.

Registry No. $[Fe(bi)_3](ClO_4)_2$, 75516-37-9.

Contribution from the Laboratory of Biological Structure, National Institute of Dental Research, National Institutes of Health, Bethesda, Maryland 20205

Lattice Defects in Nonstoichiometric Calcium Hydroxylapatites. A Chemical Approach

JOHN L. MEYER* and BRUCE O. FOWLER

Received September 25, 1981

A number of defect hydroxylapatites were prepared with Ca/P molar ratios varying from 1.40 to 1.62. These samples were analyzed for their hydroxide contents by a titration method after chemically determining their calcium, phosphate, acid phosphate, and carbonate contents. The results were compared with various general compositional formulas previously used to describe the structure and composition of the defect hydroxylapatites. Hydroxide contents between 0 and 1.13 per theoretical unit cell of hydroxylapatite, $Ca_{10}(PO_4)_6(OH)_2$, were obtained depending upon experimental conditions. The general compositional formula that best represented the experimental data was $Ca_{10-X-Y}(HPO_4)_X(PO_4)_{6-X}(OH)_{2-X-2Y}$, which describes two types of calcium vacancies in the defect lattice. The first, or X type, is coupled to the loss of a hydroxide and the addition of a hydrogen ion to the lattice and seems to be dependent upon the conditions of preparation of the precipitates. The second calcium vacancy (Y type) is electrically compensated by two vacant hydroxide positions and seems to be insensitive to solution environment with an average of about 0.5 calcium vacancy per unit cell. Other models that assume only X-type vacancies or that require one or more hydroxides for lattice stability seem to be in error.

Introduction

Hydroxylapatite (HA, $Ca_{10}(PO_4)_6(OH)_2$) serves as a model structural component for all the calcium-containing apatites of biological interest.[1] The inorganic apatitic materials present in biological hard tissue, with the possible exception of dental enamel, have carbonate-corrected calcium/phosphate molar ratios less than the theoretical 1.67, and a number of theories have been advanced to explain this discrepancy. One suggestion was that the defect hydroxylapatites (DHA) or nonstoichiometric hydroxylapatites contained the theoretical amount of hydroxide and that the low calcium phosphate ratios were due entirely to calcium ion defects with electroneutrality being maintained by the presence of two protons in the lattice for each missing calcium.[2-4] This concept results in the general formula I in Table I for the DHAs. Winand et al.[5,6] later proposed the alternative formula II, which suggests that both calcium and hydroxide defects can occur. Hydrogen ion enters the lattice in this formulation also but must necessarily be coupled with the removal of a calcium and a hydroxide ion from the lattice. Kuhl and Nebergall[7] proposed the more general formula III, which maintains electroneutrality by a combination of (a) a one-proton addition for each calcium and hydroxide defect and (b) the absence of two hydroxides per calcium ion defect. Kuhl and Nebergall[7] also allowed for the uptake of carbonate by the apatite lattice by suggesting formula IV, which substitutes CO_3^{2-} for HPO_4^{2-}. Berry,[8] using thermal and spectroscopic measurements, confirmed the general formula proposed by Winand et al.[5,6] for apatites in the Ca/P molar range 1.50–1.67 but with the added constraint that $0 \leq X \leq 1$ (formula V). Berry[9] proposed that a different formulation was required for the Ca/P molar range 1.40–1.50 (formula VI) that substitutes two hydrogen ions for each calcium as required by formula I to a lattice that contains half the theoretical hydroxide. It should be noted that Berry's[8,9] proposed structural formulas require that all DHAs contain at least 50% of the theoretical amount of lattice hydroxide. Joris and Amberg[10,11] later agreed with the two formulations proposed by Berry[8,9] on the basis of their independent measurements of the spectroscopic and catalytic properties of a number of DHAs. An alternate proposal that has received considerable attention was that the calcium defect was due to interlayered mixtures of the structurally similar octacalcium phosphate (OCP) and HA.[12,13] A general chemical formula for this system would be identical with formula II. Each of

Table I. General Compositional Formulas for Defect Calcium Hydroxylapatites

no.	formula	remarks	ref
I	$Ca_{10-X}(HPO_4)_{2X}(PO_4)_{6-2X}(OH)_2$	$0 \leq X \leq \sim 2$	2-4
II	$Ca_{10-X}(HPO_4)_X(PO_4)_{6-X}(OH)_{2-X}$	$0 \leq X \leq 2$	5, 6
III	$Ca_{10-X-Y}(HPO_4)_X(PO_4)_{6-X}(OH)_{2-X-2Y}$	$0 \leq X \leq 2$, $Y \leq 1 - X/2$	7
IV	$Ca_{10-X-Y}(HPO_4,CO_3)_X(PO_4)_{6-X}(OH)_{2-X-2Y}$	$0 \leq X \leq 2$, $Y \leq 1 - X/2$	7
V	$Ca_{10-X}(HPO_4)_X(PO_4)_{6-X}(OH)_{2-X}$	Ca/P $\geq$ 1.5, $0 \leq X \leq 1$	8, 10
VI	$Ca_{9-X}(HPO_4)_{1+2X}(PO_4)_{5-2X}(OH)$	Ca/P $\leq$ 1.5, $0 \leq X \leq 1$	9, 11

(1) McLean, F. C.; Urist, M. R. "Bone"; The University of Chicago Press: Chicago, 1961; p 148.
(2) Posner, A. S.; Perloff, A. *J. Res. Natl. Bur. Stand. (U.S.)* **1957**, *58*, 279.
(3) Posner, A. S.; Stutman, J. M.; Lippincott, E. R. *Nature (London)* **1960**, *188*, 486.
(4) Stutman, J. M.; Posner, A. S.; Lippincott, E. R. *Nature (London)* **1962**, *193*, 368.
(5) Winand, L.; Dallemagne, M. J.; Duyckaerts, G. *Nature (London)* **1961**, *190*, 164.
(6) Winand, L.; Dallemagne, M. J. *Nature (London)* **1962**, *193*, 369.
(7) Kuhl, G.; Nebergall, W. H. *Z. Anorg. Allg. Chem.* **1963**, *324*, 313.
(8) Berry, E. E. *J. Inorg. Nucl. Chem.* **1967**, *29*, 317.
(9) Berry, E. E. *J. Inorg. Nucl. Chem.* **1967**, *29*, 1585.
(10) Joris, S. J.; Amberg, C. H. *J. Phys. Chem.* **1971**, *75*, 3167.
(11) Joris, S. J.; Amberg, C. H. *J. Phys. Chem.* **1971**, *75*, 3172.
(12) Arnold, P. W. *Trans. Faraday Soc.* **1950**, *40*, 1061.
(13) Brown, W. E.; Lehr, J. R.; Smith, J. P.; Frazier, A. W. *J. Am. Chem. Soc.* **1957**, *79*, 5318.